Title	*OMC DCPD Signal Chain Analysis*
Author	*R. Abbott, Caltech*
Date	*7 April 2021*

1. Overview

Due to the redesign of the new in-vacuum preamplifiers (D2000592) various aspects of the main Gravitational Wave (GW) readout chain need to be re-examined. This note looks into the following:

- A comparison of key new and old specifications for perspective.
- Functions supported by existing and proposed in-air interface chassis.
- New vs. old whitening approach
- The sensing capability of the new bias monitors.
- The calibration chain response.

In addition to the elements above, the transition to the in-vacuum preamplifier design has the following aspects worthy of note:

- **New Design is Dual Channel** - The old preamplifiers had a single transimpedance circuit per in-vacuum box resulting in the need for two preamplifiers boxes per OMC. The new preamplifiers are dual-channel designs, thus only one in-vacuum box is needed for a direct replacement. Upon the transition to BHD readout, a second dual in-vacuum preamplifier will be needed.
- **Move Preamplifiers off the OMC Structure** - The new dual preamplifier design uses a physically large enclosure that is considerably heavier than the old design. As a consequence, it would be beneficial to move the new preamplifier design off the OMC cage (which won't even exist in 05) and onto the optical table. This will require a longer interface cable between the OMC breadboard and the preamplifier. The effects of this change must be carefully studied.
- **Fix an Inadvertent Grounding Problem** – In February of 2019, it was noted at LHO that the DCPD interface cable leading from the preamplifiers to the cable bracket on the OMC platform has an unwanted ground point as shown in the diagram below. As a new interface cable between the new dual preamplifier and the two DCPD heads is required, there is an opportunity to fix this problem (and perhaps create another). This is worth considering.

2. Product Perspective

Figure 1 Existing "Split Whitening" chassis functions

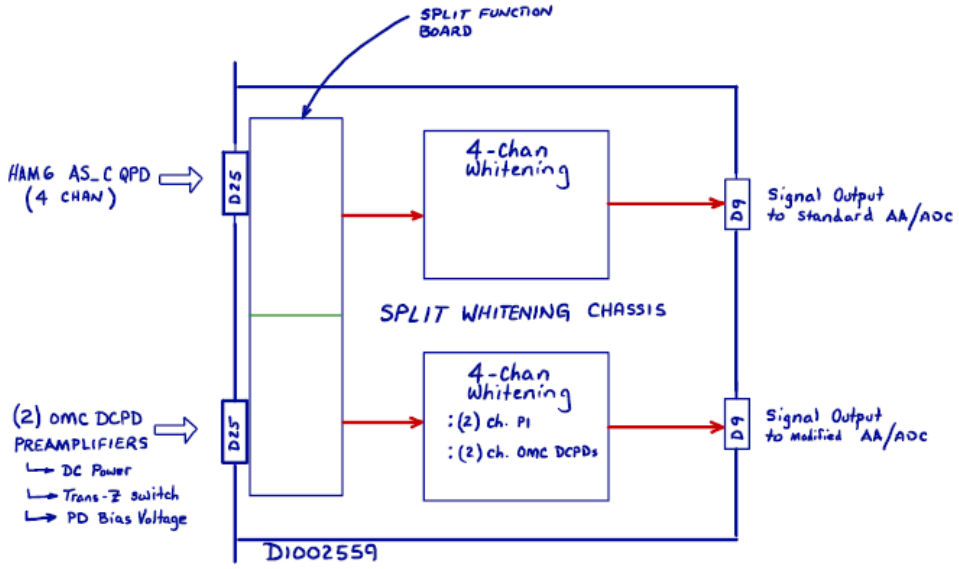

Figure 2 Inadvertent grounding associated with connector bracket on OMC Breadboard.

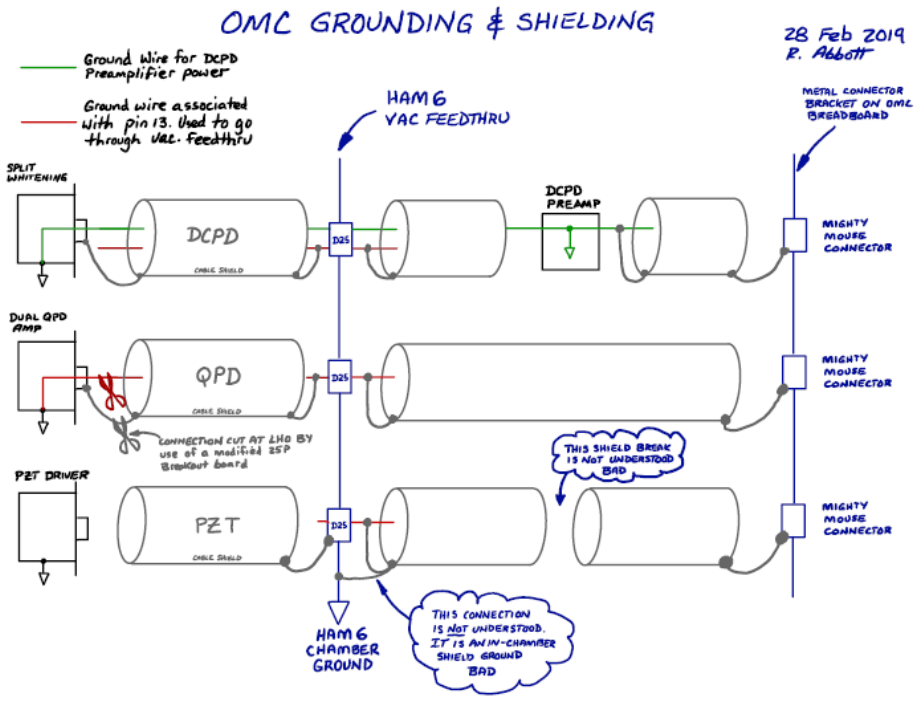

Figure 3 Existing OMC Breadboard Connector Bracket

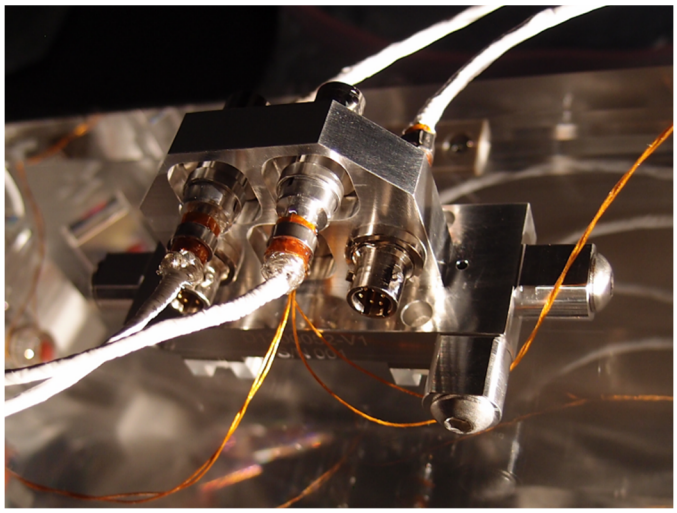

3. New vs. Old Features

Key specifications are compared below as perspective of the new and old approach to the in-vacuum preamplifier.

Parameter	Old Preamplifier	New Preamplifier
Input DC Transimpedance "seen" by photodiode	100/400 Ω	31 Ω
Overall Head DC Transimpedance	200/800 Ω	200 Ω
Overall Head Transimpedance at 50Hz	28 kΩ	102 kΩ
Overall Head Transimpedance at 1kHz	96 kΩ	99 kΩ
Overall Head Gain at 3.125MHz	391 Ω	553 Ω
SNEP at 50Hz	278uA	64uA
SNEP at 1kHz	192uA	7uA
SNEP at 3.125MHz	2.2mA	1.2mA
Head Output Voltage Noise @ 50Hz	265nV/√Hz	452nV/√Hz
Head Output Voltage Noise @ 1kHz	753nV/√Hz	149nV/√Hz
Head Input Current Noise @ 50Hz	9.4pA/√Hz	4.4pA/√Hz
Head Input Current Noise @ 1kHz	7.8pA/√Hz	1.6pA/√Hz
Input Impedance Seen by Photocurrent @ 50Hz	400Ω	220Ω
Input Impedance Seen by Photocurrent @ 1kHz	400Ω	100Ω
Transimpedance Selection	Selectable	Fixed
Calibration Path	None	Relay switchable calibration function
Bias Voltage Monitor	None	Included

4. Transfer Functions, and Noise Analysis

Figure 4 Overlay of New and Old In-vacuum Preamplifier Head Transfer Functions from Photocurrent to Differential Outputs (overall transimpedance)

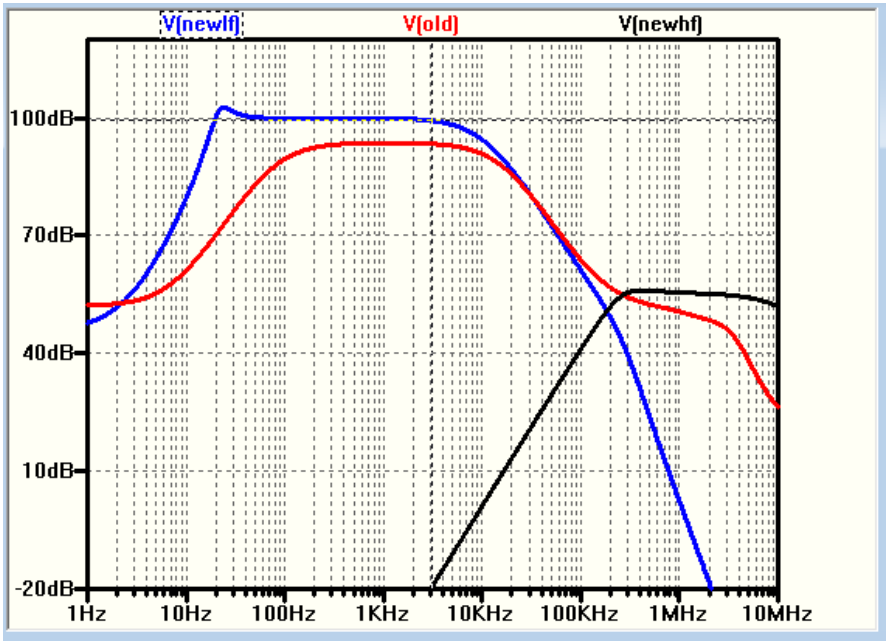

Figure 5 Old electronics chain transfer function from photocurrent to ADC input. Three filters can be switched in any combination. The first and last stages are Z=1Hz, P=10Hz. The second stage is P=50Hz, Z=500Hz. "All filters" is the normal configuration in Science Mode operations.

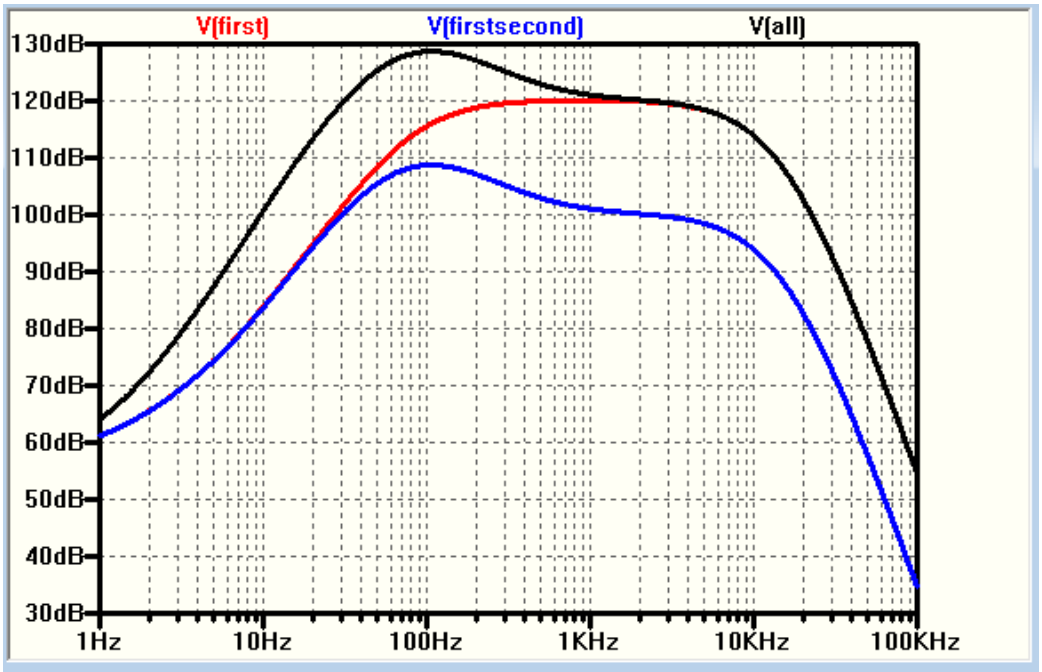

Figure 6 Predicted spectrum at input to ADC for existing (old) preamplifier design (no squeezing) using all three available stages of in-air whitening. Red curve corresponds to the signal from 10mA of photocurrent. Blue curve is the dark noise of the entire signal chain. Y-axis is in units of Vrms/$\sqrt{Hz}$

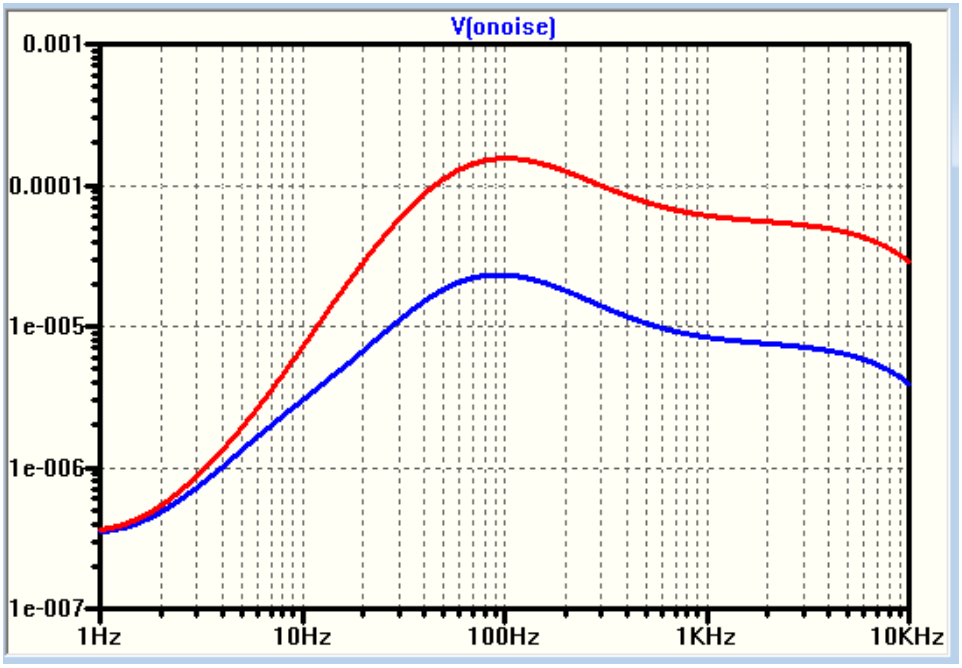

Figure 7 Predicted spectrum at differential output of new preamplifier design with 6dB squeezing applied to each shot noise curve. From top to bottom are the predicted signal levels for 30mA, 20mA, 10mA, and dark noise (blue, bottom trace). Y-axis is in units of Vrms/$\sqrt{Hz}$

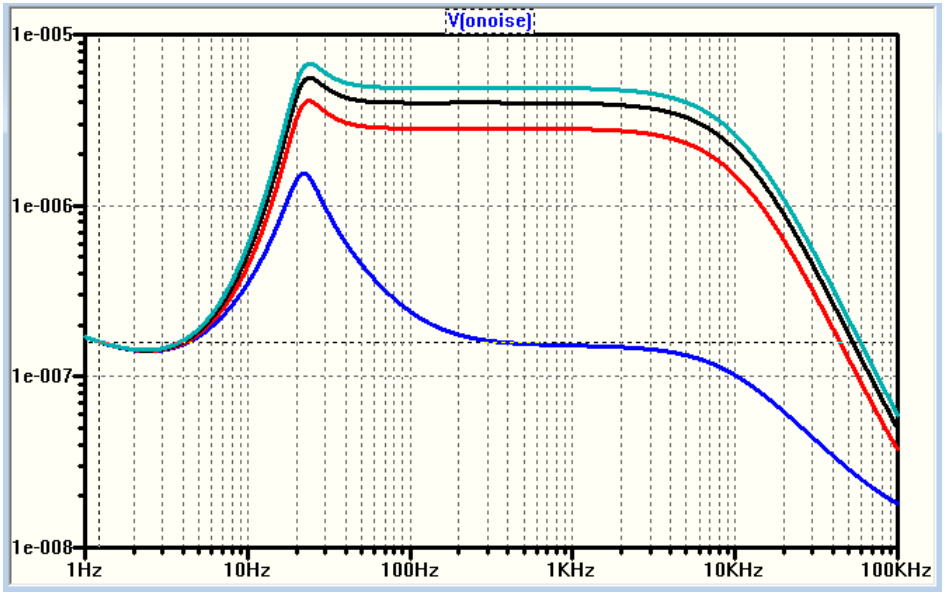

Figure 8 Bias monitor transfer function from PD to bias monitor differential output

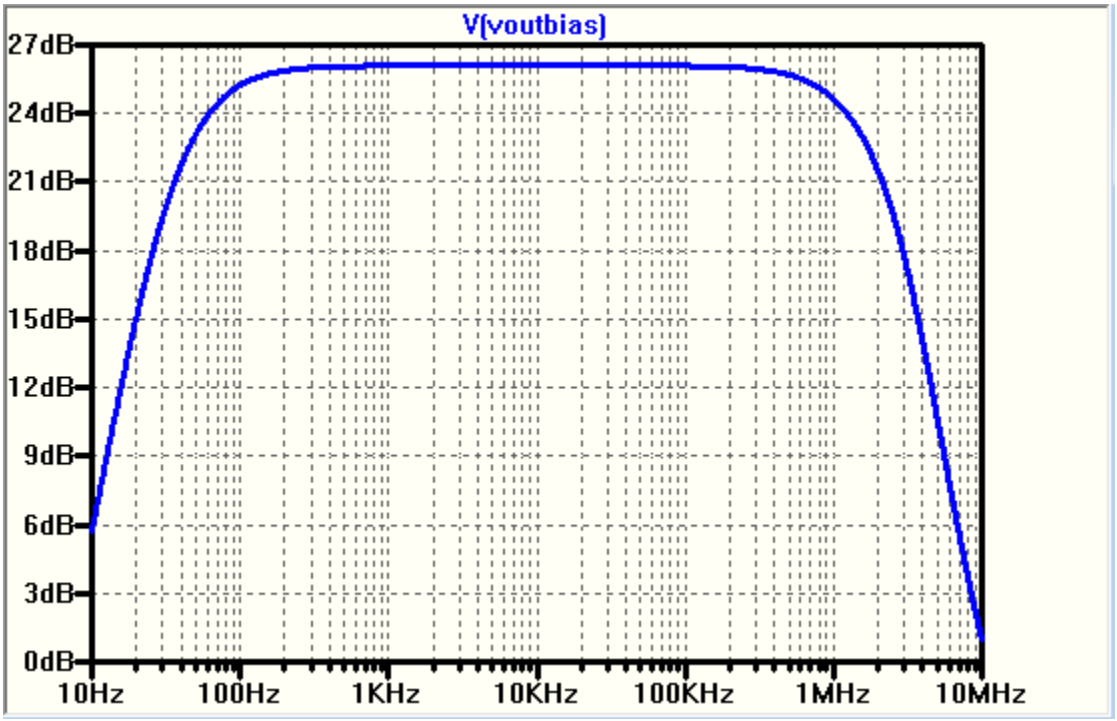

Figure 9 Approximate coupling transfer function from bias supply input to main preamplifier differential output. Useful for estimating allowable bias voltage noise.

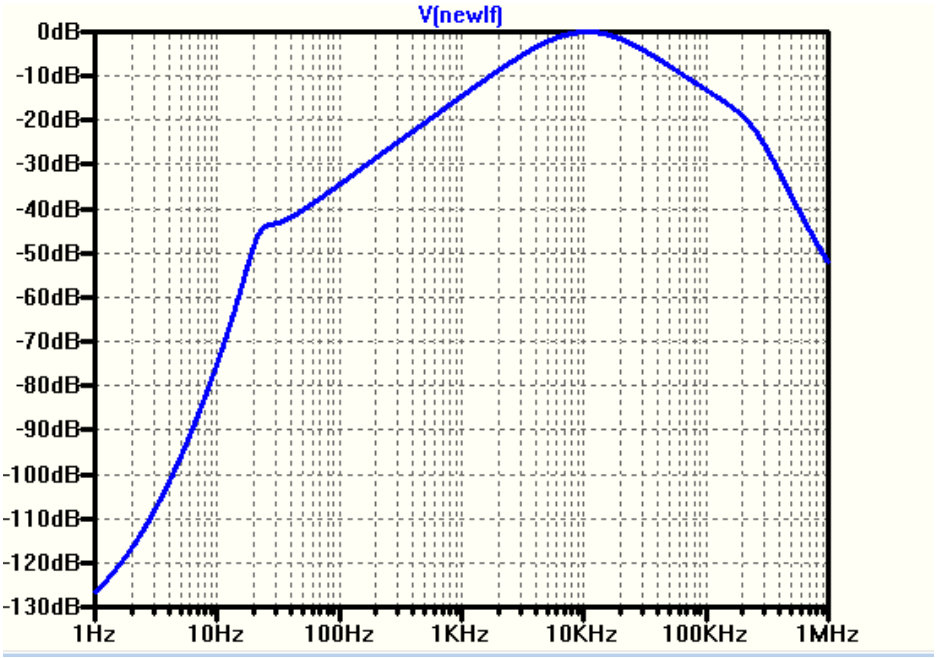

Figure 10. Bias monitor path input referred voltage noise.

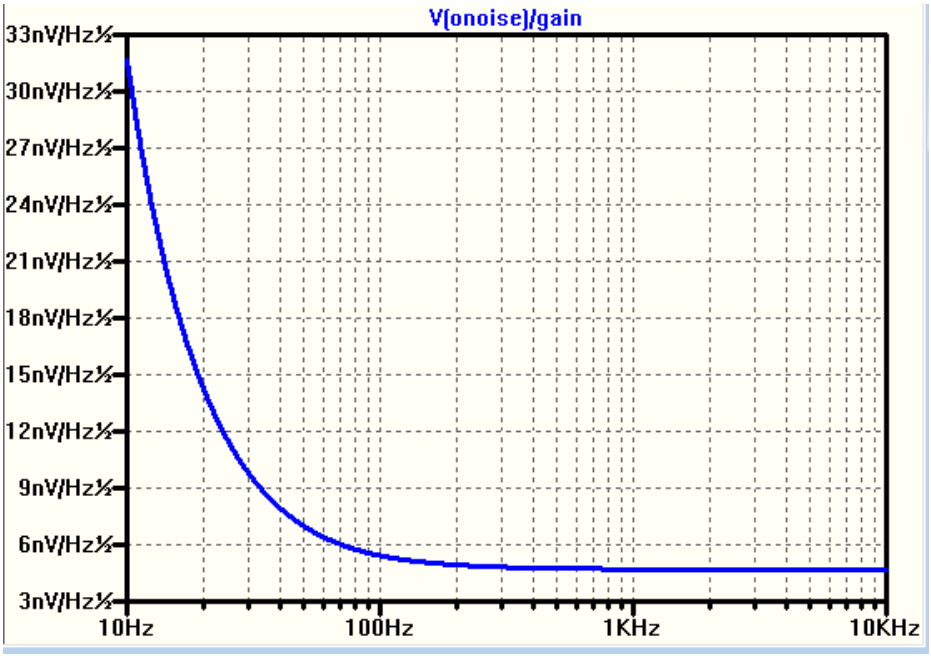

Figure 11 Calibration path transfer function assuming signal input to 100k resistor tied to PD anode, with the output taken differentially from the in-vacuum preamplifier head.

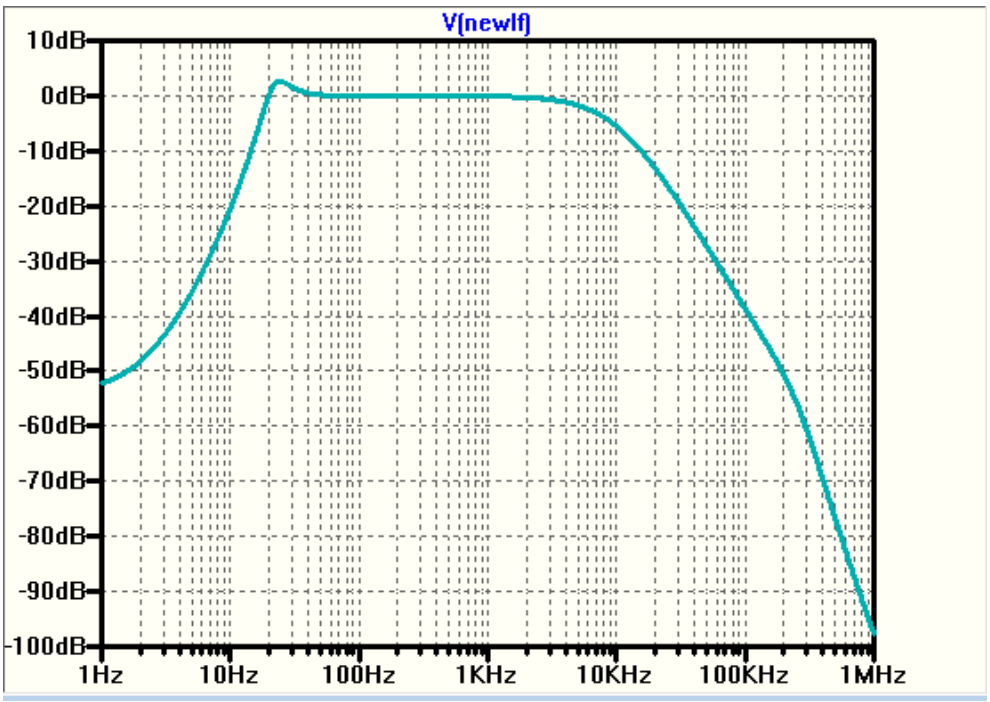

5. Required Functions for In-air Whitening and Interface Chassis

Item Number	Function
1	Filtered and current-limited source of +/-15VDC power to two dual-channel in-vacuum preamplifier heads
2	Independent on/off switch on front panel serving each in-vacuum preamplifier
3	Sufficient remotely controllable switchable whitening to support lock acquisition and normal low-noise operation for main GW outputs
4	Calibration relay on/off control (front panel and remote) with switch state readback
5	Parametric Instability (PI) signal extraction to real-time ADCs
6	Rear panel signal outputs to real-time ADC channels on Dsub connector (bias monitors, and GW output signals)
7	1U 19-inch rack mountable chassis operating on +/-18VDC raw power. Rear-panel chassis on/off switch with raw and regulated power indicating LEDs (regulated on front panel, raw on rear panel)
8	Filtered and adjustable by circuit component value choice (< tbd V/√Hz) independent source of bias voltage for each preamplifier photodiode.
9	Rear panel real-time DAC excitation input to inject calibration signals to either or both preamplifier heads. Pin-type 9-pin Dsub interface.

6. Required Whitening Implementation

The following sections describe a solution to the whitening needed to digitize the output of the new preamplifier while maintaining a specified Signal to Noise Ratio (SNR). Armed with a knowledge of the ADC input referred noise performance, the allowable SNR degradation associated with digitizing the preamplifier output time-series, and the Dark Noise associated measured at the output of the preamplifier, it is possible to calculate an ideal whitening shape which can then be approximated to facilitate the whitening filter design. Too little whitening gain will obviously degrade the SNR of the preamplifier beyond that of the allowable and inevitable degradation associated with finite input referred noise in the ADC. Conversely, too much whitening gain reduces the dynamic range overhead and renders the signal chain susceptible to saturation in the presence of fast glitches.

Figure 12 Result showing the results of a dark noise spectrum being whitened such that the dark noise equals the 16-bit ADC noise. 6dB squeezing applied to all shot noise plots.

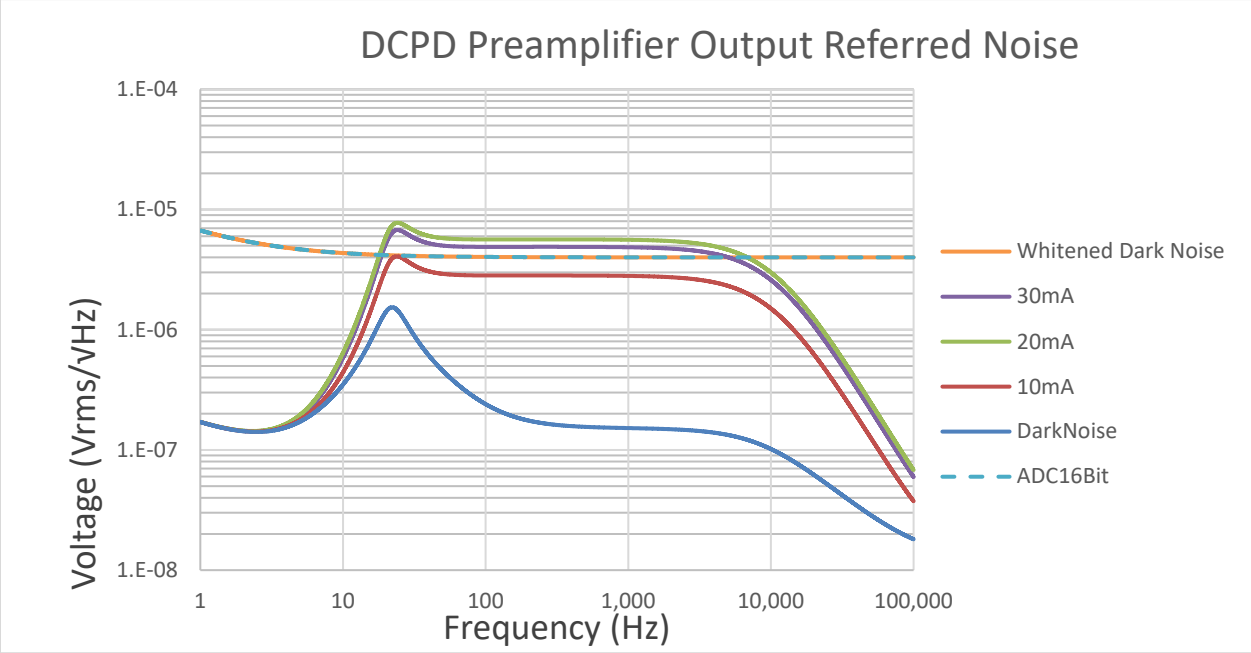

Figure 13 BLUE curve shows idealized whitening function for the dark noise to equal the 16-bit ADC noise, RED curve shows simplified approximation (2 zeros at 1Hz, 2 poles at 72Hz, 2 poles at 40kHz). This solution results in essentially the same gain as the aLIGO whitening solution. A lower noise ADC would further reduce the required gain.

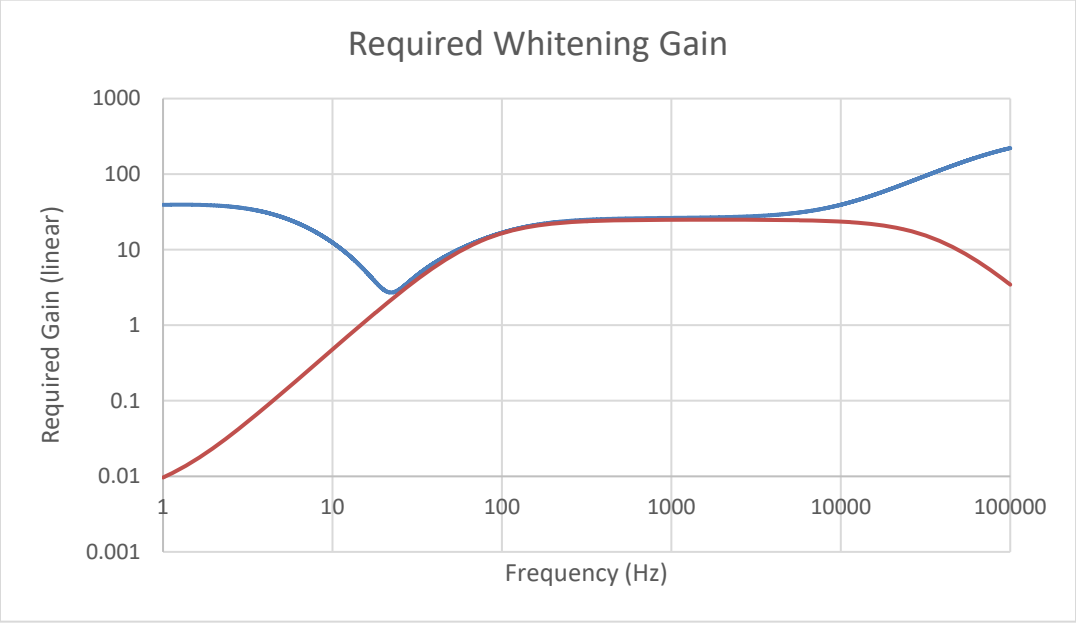

Figure 14 Overlay of the Laplace (red) and the circuit implementation (blue, two curves) for the whitening circuit only (preamp not attached). The configurations used had a 10kHz upper bandwidth limit. The blue circuit implementation shows a factor of two gain switch represented by the two blue curves.

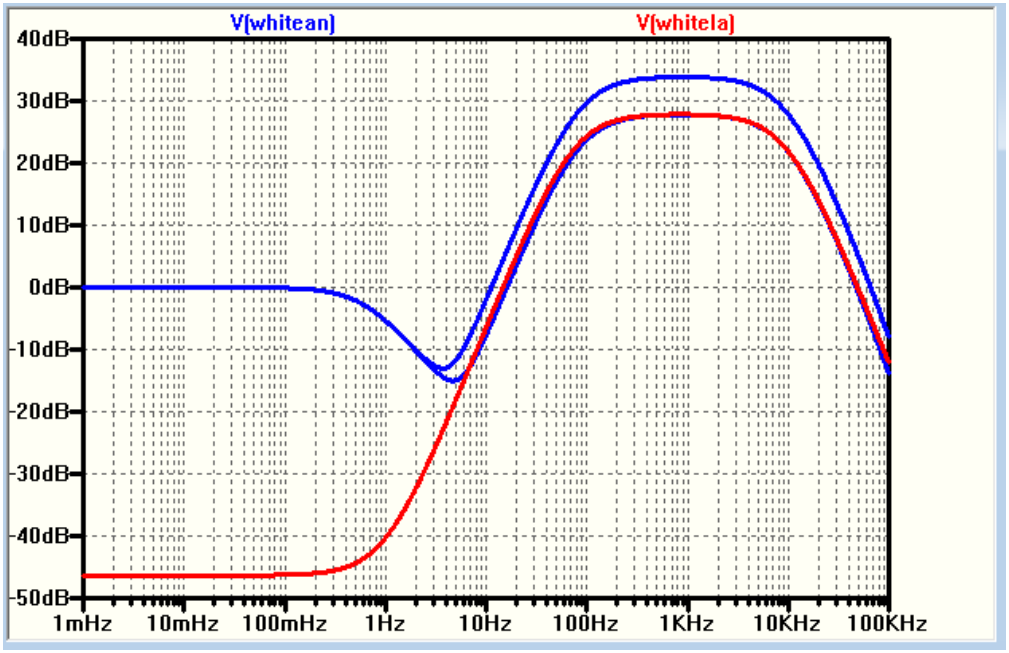

Figure 15, Transfer function of whitening solution plus new DCPD preamplifier. This shows about 128dB of total gain at 500Hz compared with 126dB gain in the previous implementation. Not far off from being the same which is deliberate to mitigate the glitch saturation tendency.

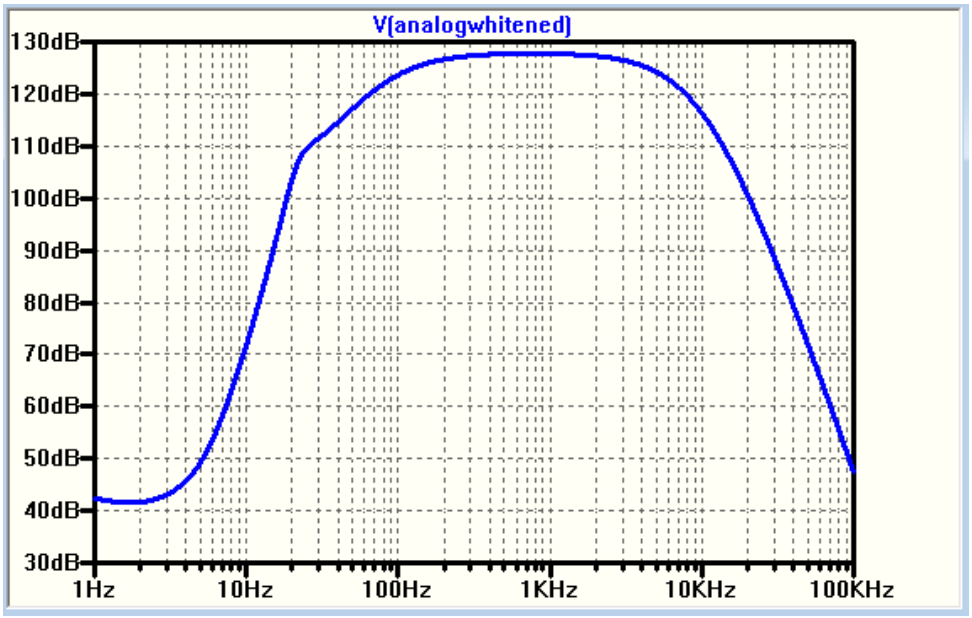

Figure 16 Preamp to PI path output. PI path taps off from the preamp output and consists of a second order Sallen-Key high-pass filter with a corner frequency of 7kHz

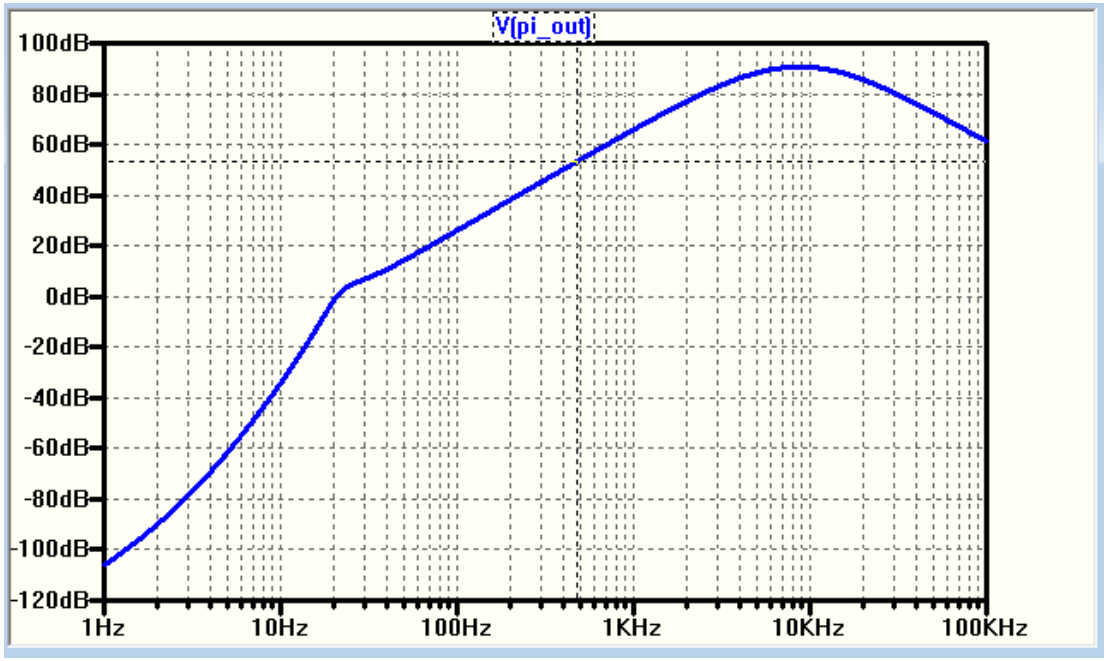

Figure 17, New Preamp and full whitening chain. Response to a 10uA spike in photocurrent. Rise and fall time are 1uSec, pulse duration 10uSec. The family of curves shows the response for an upper (analog preamp, Laplace whitening) whitening corner frequency of 40kHz, 20kHz, and 10kHz for black, red, and blue curves respectively.

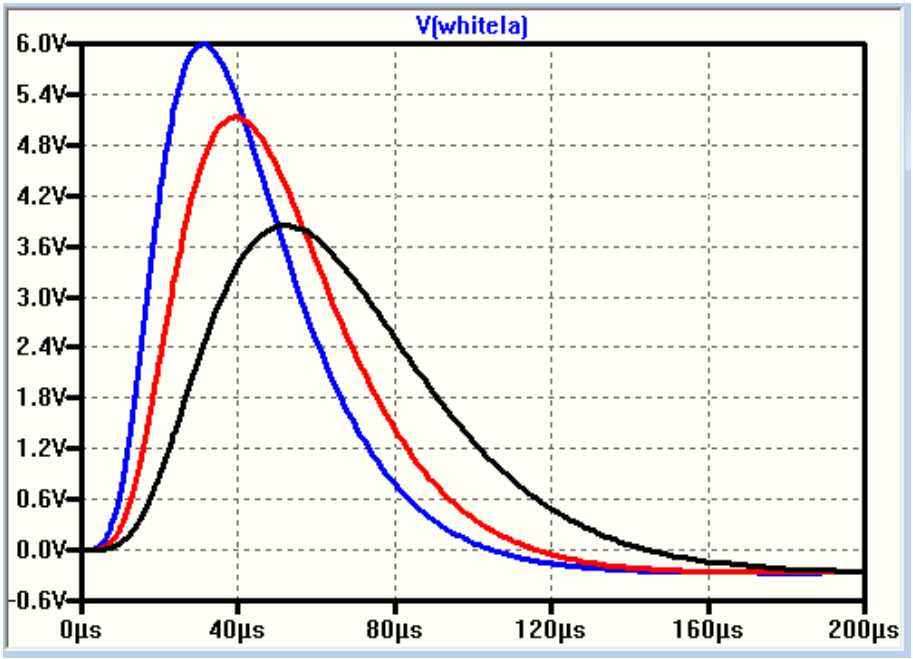

7. Circuit implementation

The circuit shown below represents an implementation of the desired whitening function for the General Standards 16-bit ADC commonly used in LIGO. A shift to a lower noise ADC can be accommodated by changing component values, but the topology will remain the same. There are several paths visible, each with points worthy of consideration

At the top of Figure 18 is a path to separate the higher frequency parametric instability signals that are commonly found in the 10kHz to 50kHz band. A second-order Sallen-Key filter is utilized to provide a 1/f2 high-pass at a corner frequency of 7kHz. It would be prudent to include a fixed gain non-inverting amplifier (not shown) in this path for gain adjustment after the filter stage implemented by U14.

The main whitening filter function is provided by opamp stages U21 and U22. The required gain is split evenly between these two stages to mitigate Gain-Bandwidth concerns. An additional stage (U9) is included to provide a switchable gain function to achieve two gain states. The whitening amplifiers and the switchable gain stage are all part of the AC coupled portion of the whitening amplifier such that the DC portion of the amplifier chain can be separately implemented. At the bottom of the figure are the idealized Laplace building blocks used to model the initial desired transfer function. An overlay of the circuit response and the ideal Laplace model shows good agreement and serves as a cross-check for the circuit implementation.

The in-vacuum preamplifier is DC coupled, so the DC information can be added back to the amplified AC signal. This is accomplished by the summing stage, U13. The ratio of the DC and AC gain can be adjusted in this path. Some rudimentary filtration has been included in the DC path by splitting the input resistor to the U13 summing stage and including a shunt capacitor. This works well and the effect is visible in the overall transfer function shown in Figure 14 as a dip in the blue curve around 4Hz to 5Hz. The only thing to keep in mind here is that the reinsertion of the DC signal must cross over with the main path at the correct phase angle for the crossover frequency used for this design. That process is simple in this case and only requires the DC to be reintroduced with a net sign inversion. Having four amplifier stages in the whitening implementation gives full freedom to adjust all of the required performance demands.

Figure 18 Schematic showing the PI path, analog version of the whitening filter, and the ideal Laplace elements used in the design.

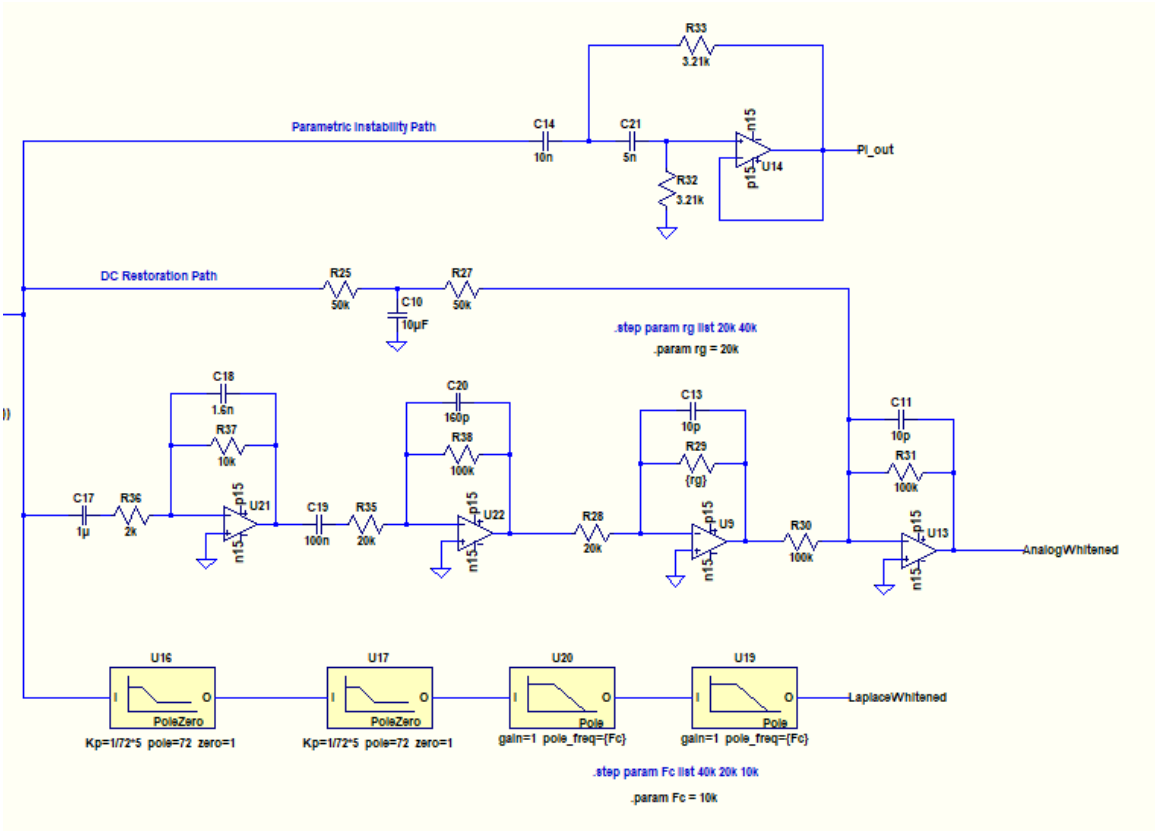

8. Scaling for Lower Noise ADCs

An ADC with improved input voltage noise performance is currently under evaluation by Valera, Keith, and Michael at LLO. The process of scaling the above results for a lower noise ADC is fairly simple, especially if the shape of the noise spectrum is similar in terms of the 1/f noise corner frequencies. The required gain curve in Figure 13 would shift representing a lower requirement for the whitening gain. This in turn lowers the tendency for glitches in photocurrent to cause saturations in the whitening amplifier chain.

9. How to Calculate the Ideal Whitening Transfer Function

Figure 19, Calculation Notes

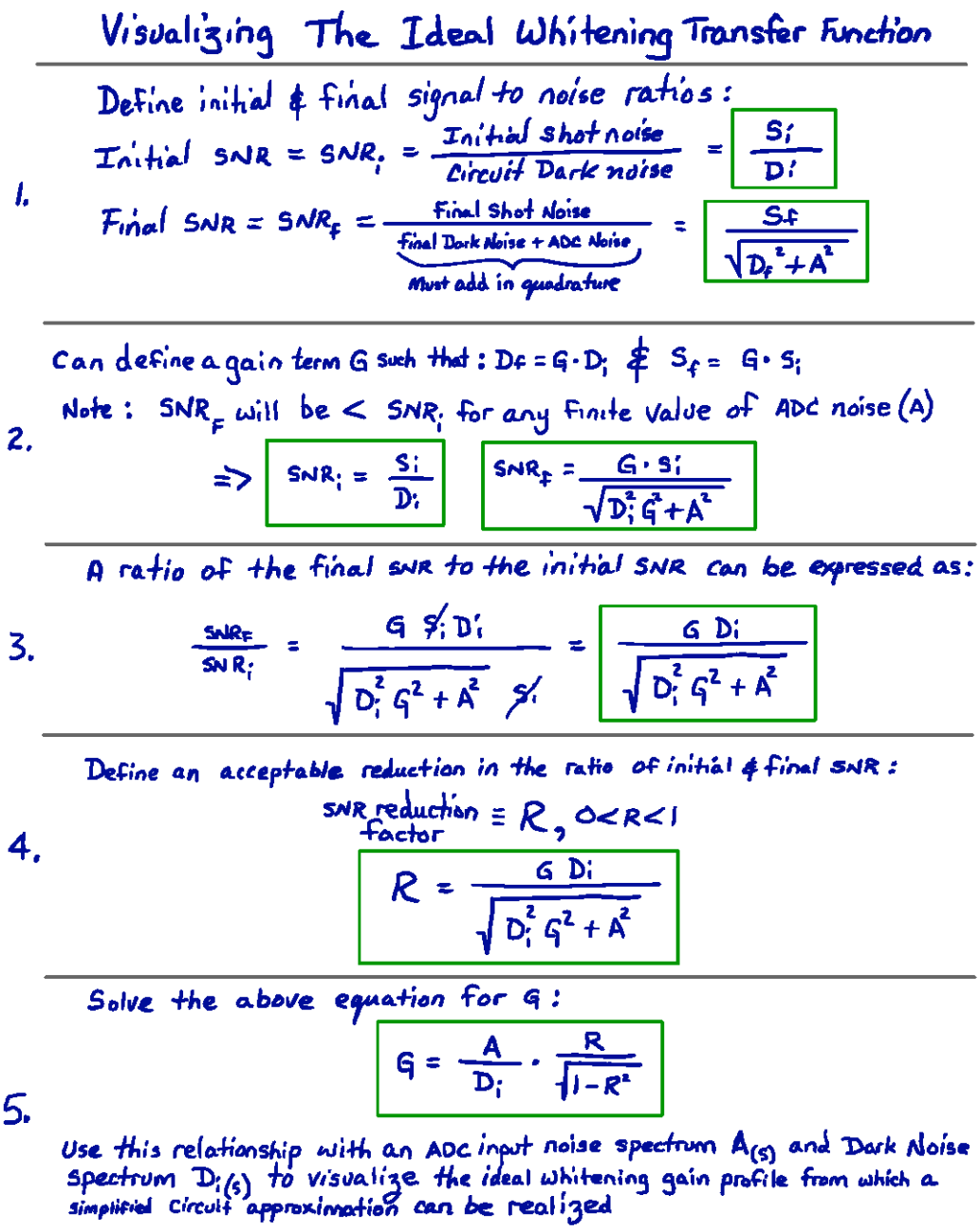

Visualizing The Ideal Whitening Transfer Function

1. Define initial & final signal to noise ratios:

Initial SNR = $SNR_i = \frac{\text{Initial shot noise}}{\text{Circuit Dark noise}} = \boxed{\frac{S_i}{D_i}}$

Final SNR = $SNR_f = \frac{\text{Final Shot Noise}}{\underbrace{\text{final Dark Noise + ADC Noise}}_{\text{Must add in quadrature}}} = \boxed{\frac{S_f}{\sqrt{D_f^2 + A^2}}}$

2. Can define a gain term G such that: $D_f = G \cdot D_i$ & $S_f = G \cdot S_i$

Note: SNR_F will be < SNR_i for any finite value of ADC noise (A)

$\Rightarrow$ $\boxed{SNR_i = \frac{S_i}{D_i}}$ $\boxed{SNR_f = \frac{G \cdot S_i}{\sqrt{D_i^2 G^2 + A^2}}}$

3. A ratio of the final SNR to the initial SNR can be expressed as:

$$\frac{SNR_F}{SNR_i} = \frac{G \cancel{S_i} D_i}{\sqrt{D_i^2 G^2 + A^2}\ \cancel{S_i}} = \boxed{\frac{G D_i}{\sqrt{D_i^2 G^2 + A^2}}}$$

4. Define an acceptable reduction in the ratio of initial & final SNR:

SNR reduction factor $\equiv R$, $0 < R < 1$

$$\boxed{R = \frac{G D_i}{\sqrt{D_i^2 G^2 + A^2}}}$$

5. Solve the above equation for G:

$$\boxed{G = \frac{A}{D_i} \cdot \frac{R}{\sqrt{1 - R^2}}}$$

Use this relationship with an ADC input noise spectrum $A_{(s)}$ and Dark Noise spectrum $D_{i(s)}$ to visualize the ideal whitening gain profile from which a simplified circuit approximation can be realized